Low-pressure oligomerization of diluted ethylene on a HZSM-5 zeolite catalyst

Zuria Tabernilla [*], Ainara Ateka, Andrés T. Aguayo, Javier Bilbao, Eva Epelde [**]

Department of Chemical Engineering, University of the Basque Country (UPV/EHU), P. O. Box 644, 48080, Bilbao, Spain

ARTICLE INFO

ABSTRACT

The oligomerization at low pressure of diluted ethylene coming from secondary streams is an attractive route for hydrocarbon production, by means of a low cost and energy efficient process. To evaluate the viability of this process, the effect of dilution with N_2 or syngas on the low-pressure oligomerization of ethylene (1.5 bar) was studied on a catalyst prepared with a HZSM-5 zeolite agglomerated in a mesoporous matrix of α- and γ-Al_2O_3, aiming to produce C_{5+} hydrocarbons (gasoline). The experiments were performed in a fixed bed reactor at 325 °C and a space time of 10.6 $g_{catalyst}$ h mol_C^{-1}. For an ethylene partial pressure of 0.33 bar, conversion surpassed 80 % and high C_{5+} hydrocarbon yield was obtained: >40 % with N_2 as diluent; and, >30 % with syngas. The greater effect of syngas dilution on suppressing the formation of aromatics is explained by the role of H_2 in decreasing the extent of dehydrocyclization reactions. The dilution of ethylene limits the extent of the reaction stages, but it also attenuates the stages for coke formation, by facilitating the diffusion of soft coke in the mesoporous matrix and contributing to decrease the deposition of hard coke in the zeolite micropores. Consequently, a pseudo-steady state of the catalyst is reached with a notable remnant activity for the formation of higher hydrocarbons.

1. Introduction

In the transition period towards the general use of renewable energies, the fulfillment of the decarbonization commitment by the developed countries calls for the improvement of new processes to produce fuels and chemicals from sustainable sources and to intensify the valorization of fossil fuels (Rissman et al., 2020; Zhang et al., 2022). In this scenario, the oligomerization of light olefins to liquid fuels is presented as an attractive opportunity to valorize streams in which these olefins are present, although their dilution makes uneconomical their separation to be used as feedstock in the synthesis of polyolefins. This situation is related to surplus gas streams in natural gas (Ghashghaee, 2018) and dry gas from refinery fluidized catalytic cracking (FCC) units (Palos et al., 2020), where the destination of the diluted ethylene present is energy recovery. Similarly, in the fast pyrolysis of polyolefinic plastics, the light olefins produced are diluted in the N_2 used as inert gas (Artetxe et al., 2012). Also, in the hydrogenation of syngas or CO_2 to olefins (by the modified Fischer-Tropsch routes and with methanol as intermediate), light olefins are diluted with H_2, CO, CO_2 and methane (Portillo et al., 2022). Additionally, ethylene is also diluted in the

oxidative coupling of methane (OCM) product stream (Liu et al., 2022). The on-line oligomerization of ethylene in these streams into liquid fuels, without the inherent costs of separation and avoiding compression, is an interesting initiative in the context of process intensification strategies, with the improvement of energy efficiency and its economy as main goals (Kriván et al., 2016; Moioli, 2022).

The technologies for the oligomerization of light olefins operate at elevated pressure, and among them, the one based on the use of HZSM-5 based catalysts is well established, with the historical reference of the Mobil Olefins to Gasoline and Distillate (MOGD) process (Quann et al., 1988; Tabak et al., 1986). The characteristic micropores of the MFI structure of HZSM-5 zeolite (with a high degree of connection between the channels and without cages in the intersections) facilitates the diffusion of light olefins and the development of the carbocationic mechanism of oligomerization, by also limiting the confinement of the oligomers. In addition, the acidity of the HZSM-5 zeolite can be modulated to favor the selective production of higher olefins or fuels with a reduced content of aromatics (Mlinar et al., 2012; Corma et al., 2013). To explain the role of the acid sites, Jin et al. (2021) proposed a detailed kinetic model, where the activity of the zeolite for the individual

---

reactions is related to the presence of acid sites of different acidic strength.

The aforementioned studies in the oligomerization of ethylene have been performed at high pressure and by paying little attention to catalyst deactivation. Studies of ethylene oligomerization at low pressure and with presence of diluents haven been mainly directed to the conversion of bioethanol into hydrocarbons, where ethylene is considered as a real reactant because it is rapidly formed at the reactor inlet by dehydration of bioethanol. These studies have shown the notable impact of dilution on product distribution and on catalyst deactivation (Gayubo et al., 2001; Aguayo et al., 2002; Ding et al., 2009; Andrei et al., 2020; Fernandes et al., 2020, 2021). Through the characterization of the occluded intermediates (Johansson et al., 2009) and with different techniques (isotopic labeling, temporal analysis of products, and ab initio microkinetic modeling) (Van der Borght et al., 2016; Batchu et al., 2017; Zeng et al., 2022), a dual cycle mechanism, similar to that established for the conversion on methanol to hydrocarbons, with olefins and aromatics (alkylbenzenes) as intermediates in each cycle, has been justified for bioethanol conversion.

Particularly, ethylene conversion to higher hydrocarbons is hindered by the limited reactivity of this olefin, which is lower than that of other olefins of higher molecular weight (Garwood, 1983). Therefore, a higher temperature is needed than the one required for the oligomerization of propylene or butenes, which favors the extent of secondary reactions of cracking and coke deposition. Consequently, a challenge in the oligomerization of ethylene on HZSM-5 based catalysts is the attenuation of catalyst deactivation. The cause of this deactivation is the retention of oligomers in the micropores of the catalyst and their evolution towards polyaromatic structures, blocking the acid sites and micropores of the zeolite (Monama et al., 2020). In a previous study (Díaz et al., 2020a) the good behavior of a HZSM-5 based catalyst with a hierarchical porous structure in the oligomerization of 1-butene at 1.5 bar was studied.

In this work the oligomerization of ethylene diluted with N_2 or with syngas has been studied at reduced pressure (1.5 bar) aiming to determine the effect of ethylene partial pressure and of the nature of the diluents on the conversion and yield of the product fractions, and on the deactivation of the catalyst (a HZSM-5 zeolite agglomerated in a mesoporous matrix). It has been previously proven that the presence of the matrix is a key feature to improve the stability of the HZSM-5 zeolite (Díaz et al., 2020b; Tabernilla et al., 2023), whose overall good performance in the oligomerization of light olefins is well established in the literature (Li et al., 2017; Chen et al., 2020). It is remarkable that the presence of a mesoporous matrix facilitates the diffusion of the oligomers towards the exterior of the catalyst particle, by avoiding the total blockage of the zeolite micropores and attenuating the extent of oligomer condensation into polyaromatic structures of hard coke. This effect of the matrix enables the catalyst to reach a pseudo-steady state with a substantial remnant activity, as it has been previously proven in the conversion of oxygenates into olefins (Pérez-Uriarte et al., 2016) and in the oligomerization of 1-butene (Díaz et al., 2021). Special attention has been paid in this work to the production of C_{5+} hydrocarbons and to their composition, due to the interest of being added into the refinery gasoline pool. The monitoring of the evolution of the results with the time on stream and the analysis of the nature and location of the coke has allowed to determine the effect of the dilution on attenuating the deactivation and on facilitating a pseudo-steady state of the catalyst with remarkable activity. The results are of interest for the valorization of diluted ethylene-containing streams from different processes for hydrocarbon production from sustainable sources.

2. Experimental

2.1. Catalyst preparation and characterization

The procedure for catalyst preparation and characterization is reported in detail elsewhere (Díaz et al., 2020b; Tabernilla et al., 2023). In the preparation of the catalyst, a HZSM-5 zeolite (Zeolyst International, SiO_2/Al_2O_3 molar ratio of 30) was agglomerated with pseudoboehmite (Sasol Germany, 32 wt%) as binder and a colloidal dispersion of α-Al_2O_3 (Alfa Aesar, 18 wt%) as inert filler. It should be mentioned that the colloidal nature of the filler facilitates the preparation by increasing the homogeneity of the mixture. The catalyst particles were obtained by extrusion of the mixture of these materials, and the extrudates were first dried at room temperature (24 h) and later in an oven at 110 °C (24 h). Subsequently, the particles were sieved to a particle size range between 0.12 and 0.3 mm (suitable for its use in a fixed bed reactor). Prior to its use, the catalyst is calcined at 575 °C for 2 h (heating ramp of 5 °C min^{-1}). After this calcination, the zeolite adopts its acid form and it is hydrothermally stable (property required to recover its acidity in successive reaction-regeneration cycles for coke combustion). Moreover, during this calcination step the pseudoboehmite is converted into γ-Al_2O_3. Note that the method for the agglomeration of the zeolite and the nominal composition of the composite (50 wt% zeolite/32 wt% γ-Al_2O_3/18 wt% α-Al_2O_3) is suitable to obtain a high mechanical strength, by almost keeping zeolite properties (Pérez-Uriarte et al., 2016). Thus, a higher content of binder and filler gives way to a substantial decrease in zeolite properties, due to the partial blockage of the micropore mouths.

The physical properties (BET surface area, micro- and mesopore volume and distribution) and the acid properties of the fresh zeolite, the matrix and catalyst are shown in Table 1. The properties of the matrix gathered in Table 1 correspond to a composite of γ-Al_2O_3/α-Al_2O_3, prepared by the former procedure for catalyst preparation, but in the absence of zeolite. The physical properties were determined by N_2 adsorption-desorption (Fig. S1 in the Supporting Information) in a Micromeritics ASAP 2010. The acid strength of the catalyst was determined by adsorption-desorption of NH_3 in a calorimeter Setaram TG-DSC 111, with a Harvard injection pump, coupled to a mass spectrometer Balzers Instruments. Prior to analysis, the samples were swept with He (80 cm^3 min^{-1}) at 500 °C for 1 h. Then, the temperature was stabilized at 150 °C with a flow rate of He of 20 cm^3 min^{-1}. At these conditions, the saturation of the sample was carried out by injection of NH_3 (50 cm^3 min^{-1}). After the saturation of the sample, the physically adsorbed molecules were removed with He (20 cm^3 min^{-1}) at 150 °C. Finally, a temperature-programmed desorption (TPD) was performed by heating up the sample up to 550 °C with a heating rate of 5 °C min^{-1} in a flow rate of He of 20 cm^3 min^{-1}, recording at the same time the signal of NH_3. The procedure was also reproduced in an Autochem 2920 equipment to ascertain the NH_3-TPD profiles (Fig. S2).

In order to deepen in the identification of the type of acid sites in the samples (Brønsted and Lewis acid sites) pyridine adsorption was carried out at 150 °C using a Nicolet 6700 apparatus equipped with a Specac catalytic chamber. A tablet of ~10 mg of sample (zeolite or catalyst) was prepared by grinding and pressing the grains at 10–12 ton cm^{-2} for 15 min. The tablet was introduced in the catalytic chamber and was submitted to a heat pretreatment at 550 °C with a heating rate of 10 °C min^{-1}, under vacuum, to eliminate impurities. Then, temperature was cooled down to 150 °C and the signal was recorded with a frequency of 2 min^{-1}. The results are gathered in Fig. S3.

Table 1

Physical and acid properties of the matrix, HZSM-5 zeolite and catalyst.

	Matrix	Zeolite	Catalyst
Physical properties			
S_{BET} (m^2 g^{-1})	147	356	281
S_{micro} (m^2 g^{-1})	0	275	160
V_{meso} (cm^3 g^{-1})	0.41	0.11	0.30
V_{micro} (cm^3 g^{-1})	0	0.11	0.07
Acid properties			
Total acidity (μmol $_{NH3}$ g^{-1})	107	686	362
Acid strength (kJ mol$_{NH3}^{-1}$)	50	150	110
BAS/LAS ratio	0	4.3	3.4

As observed in Table 1, the presence of the matrix increases the pore volume with respect to the zeolite due to the contribution of the matrix mesopores. Furthermore, the impact of the matrix on the acidity is the decrease of the total acidity and the average acid strength of the sites, due to the limited acidity of the sites (weak only) of the γ-Al_2O_3 in the matrix.

2.2. Reaction equipment and conditions

Ethylene oligomerization runs were carried out in a reaction equipment shown in Fig. S4 and described in detail elsewhere (Tabernilla et al., 2023). The reactor is a 316 stainless-steel fixed-bed reactor (internal diameter of 9 mm and an effective length of 100 mm). To ensure a constant height of 1.5–2 cm, the catalytic bed is formed of catalyst and inert solid (SiC). To avoid condensation problems, the gas product stream is heated up to 110 °C and it is analyzed online in an Agilent 300A MicroGC gas-chromatograph, which is equipped with the following columns: i) Molecular sieve (MS-5A) to quantify O_2, N_2, H_2, CO, CH_4, CO_2; ii) Porapak Q (PPQ) for oxygenated compounds, CO_2, light olefins ($C_2^=$-$C_3^=$) and water; iii) Alumina for light hydrocarbons up to C_4, and; iv) OV-1 type column for higher hydrocarbons. Gas product stream was analyzed every 4 min. Liquid products (C_5–$C_{20,}$ with insignificant contents of retained C_3 and C_4 compounds) collected in different periods of time on stream were analyzed ex-situ in a GC × GC/MS (Agilent 5975C Series GC/MSD) equipment coupled on-line with an XL MSD mass spectrometer equipped with a FID detector, a non-polar column (DB-5MS, 30 m × 0.25 mm × 0.25 μm), and a polar column (HP-INNOWAX, 5 m × 0.25 mm × 0.15 μm). For the analysis a 2 °C min^{-1} heating rate was used from 40 °C to 200 °C (constant for 4 min). Detailed information on the analysis is described in Section S3 in the Supporting Information.

Typically, the reactions were carried out at: 1.5 bar; 325 °C; space time, 10.6 $g_{catalyst}$ h mol_C^{-1} (corresponding to a catalyst mass of 1 g and an ethylene molar flow rate of 37 ml min^{-1}); ethylene concentration in the feed, 20–80 % (using 99.999 % ethylene, Air Liquide); ethylene partial pressure in the feed, 0.33–1.18 bar, using as diluents N_2 and syngas (H_2/CO molar ratio of 3/1); and, time on stream (TOS), 5 h. These conditions have been established based on the results obtained in a prior work where the same catalyst was used in the oligomerization of pure ethylene (Tabernilla et al., 2023).

The results were evaluated in terms of ethylene conversion (X), yield (Y_i) and selectivity (S_i) of each lumped product, which are defined in Eqs. (1)–(3), respectively.

$$X = \frac{F_0 - F}{F_0} \cdot 100 \tag{1}$$

$$Y_i = \frac{F_i}{F_0} \cdot 100 \tag{2}$$

$$S_i = \frac{F_i}{F_0 - F} \cdot 100 \tag{3}$$

where F_0 and F, are the molar flowrate of ethylene in the feed and in the outlet stream, while F_i is the flowrate of i lump in the outlet stream. All flowrates in Eqs. (1)–(3) are expressed in content C units.

The following main lumps have been defined: $C_3^=$ and $C_4^=$ olefins, C_4 paraffins, C_{5-7} aliphatics (mainly paraffins) and C_{5+} (gasoline) fraction (including olefins, paraffins and aromatics). No methane has been detected under the operating conditions studied.

2.3. Used catalyst characterization

After each reaction, the catalytic bed was swept with 30 cm^3 min^{-1} of N_2 at the reaction temperature (325 °C) for 30 min in order to ensure the reproducibility of the used catalyst characterization analyses. The content and nature of the different types of coke (soft coke and hard coke) were determined by temperature-programmed sweeping with N_2 (N_2-TPS) followed by temperature-programmed oxidation (TPO) analysis, respectively, using a TGA Q5000TA thermobalance (Thermo Scientific) equipment.

For the N_2-TPS analysis, the used catalyst samples (~15 mg) were treated with N_2 (50 cm^3 min^{-1}) heating up the sample up to 350 °C with a heating rate of 10 °C min^{-1} and kept for 20 min, to sweep the soft coke confined in the catalyst pores. Subsequently, the TPO analyses of the remaining coke fraction (hard coke) were carried out with air (50 cm^3 min^{-1}), up to 700 °C (2 °C min^{-1}) and kept for 1 h (to ensure the complete combustion of the hard coke formed inside the zeolite channels).

3. Results

3.1. Conversion and product yield

Fig. 1 shows the effect of ethylene partial pressure in the reactor inlet feed, diluted in N_2 (Fig. 1a) and in syngas (SG) (Fig. 1b), on ethylene conversion and product yield ($C_3^=$ and $C_4^=$ olefins, C_4 paraffins, C_{5-7} aliphatics (mainly paraffins), and C_{5+} (gasoline) hydrocarbons) at zero time on stream (first sampling at 4 min). An increase in ethylene partial pressure in the feed upturns the conversion (above 80 % at all conditions), which is coherent with the literature on the conversion of light olefins on HZSM-5 catalysts, by increasing the same variable (Lin et al., 2009; Fernandes et al., 2020), or the absolute pressure (Ding et al., 2009). The increase of ethylene conversion caused by a raise in ethylene partial pressure is associated with a greater amount of reagent available at zeolite active sites. The main difference between the results with the two diluents is that with syngas dilution (Fig. 1b) the complete conversion is not reached and the yield of C_{5+} hydrocarbons is notably lower. Considering that the yield of C_{5-7} aliphatics is similar, the difference in the yield of C_{5+} hydrocarbons is due to the attenuation of aromatic formation with syngas as diluent. The explanation lies in the attenuation of the extent of the dehydrocyclization reactions of ethylene, propylene and butenes, the latter two having a relevant role as highly reactive intermediates in the oligomerization of ethylene over HZSM-5 catalysts (Fernandes et al., 2020).

For both diluents, the yield of butenes ($C_4^=$, formed by ethylene dimerization and intermediates in the formation of higher olefins) and propylene ($C_3^=$, product of cracking by β-scission of higher oligomers) decreases with increasing ethylene partial pressure in the reactor inlet stream. It should be noted that this effect of ethylene partial pressure is used to maximize propylene selectivity from ethylene conversion on HZSM-5 catalysts (Lin et al., 2009).

3.2. Catalyst deactivation

Under kinetic regime conditions (not excess of catalyst), ethylene conversion decreases with time on stream due to catalyst deactivation. Increasing ethylene partial pressure in the feed, it is observed that under these conditions the deactivation is faster, being this effect more relevant in Fig. 2b (with syngas as diluent) than in Fig. 2a (with N_2). This effect cannot be observed in Fig. 2 as the decrease in conversion is insignificant. However, it is more evident on the evolution of product distribution (Fig. 3) as later commented. The increase in the deactivation rate is explained because an increase in ethylene partial pressure favors the extent of the formation of oligomers that are retained in the pores of the catalyst, and thus, the extent of reactions for coke formation, as checked in Section 3.4.

A slightly lower deactivation was also observed with H_2 as diluent, which can be attributed to the role of H_2 in attenuating the rate of dehydrocyclization reactions of olefins with formation of coke. It should be noted that Andrei et al. (2020) observed a more important effect of deactivation attenuation in the oligomerization of diluted ethylene by the presence of H_2, but working at 15 bar. In Section 3.2 an explanation
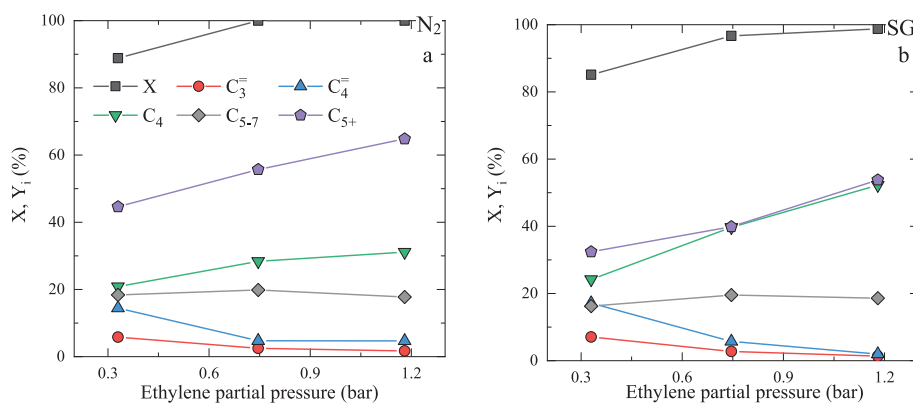
Fig. 1. Effect of ethylene partial pressure in the feed on its conversion and on the yield of the main lumped products for different diluents: a) N_2 and b) Syngas (SG). Reaction conditions: 325 °C; 1.5 bar; space time, 10.6 $g_{catalyst}$ h mol_C^{-1} (1 g of catalyst); 0 h on stream.
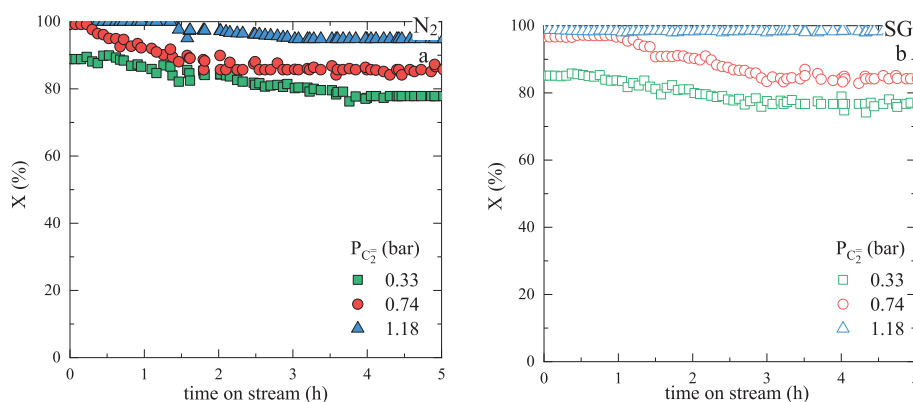

Fig. 2. Effect of ethylene partial pressure in the feed on the evolution with time on stream of ethylene conversion for different diluents a) N_2 and b) Syngas (SG). Reaction conditions: 325 °C; 1.5 bar; space time, 10.6 $g_{catalyst}$ h mol_C^{-1} (1 g of catalyst).

on deactivation is given, in which the role of occluded oligomers and coke of catalytic origin are distinguished.

It is remarkable in the dynamics of deactivation in Fig. 2 that after an initial period of rapid deactivation the conversion results in Fig. 1 are almost constant. In the initial rapid deactivation, the oligomers occluded in the catalyst block the access of ethylene and of the reaction intermediates to the zeolite micropores, and so, hamper the formation and subsequent diffusion of the oligomers towards the exterior (Mlinar et al., 2012; Díaz et al., 2020a; Bickel and Gounder, 2022). Aiming to minimize the deactivation in this initial period, Corma et al. (2013) checked for the interest of generating mesopores within the zeolite to attenuate the blockage of the micropores. The presence of a mesoporous matrix is disclosed as an efficient strategy for the diffusion of the oligomers towards the exterior of the catalyst particle (Díaz et al., 2021). The results in Fig. 2 show the effectiveness of zeolite agglomeration in a mesoporous matrix to minimize the initial deactivation by pore blockage, which enables to reach a pseudo-steady state of the catalyst with a remarkable remnant activity. Under this state, the deactivation of the catalyst is slow and it is related to the evolution of the retained oligomers towards polyaromatic condensed coke structures through condensation reactions (Halmenschlager et al., 2016). These reactions are catalyzed by acid sites, where Brønsted sites play a key role (Zhang et al., 2020), by the well-established mechanisms with aromatics as main intermediates (Guisnet and Magnoux, 2001; Chung et al., 2011; Ibáñez et al., 2017; Cordero-Lanzac et al., 2018). In Fig. S5 the evolution of ethylene conversion is compared for the zeolite and the agglomerated catalyst.

The effect of ethylene dilution on the evolution with time on stream of the main product distribution is shown in Fig. 3 (for N_2 as diluent) and Fig. 4 (for syngas). As observed, this dilution attenuates catalyst

deactivation and it has an impact on product distribution, due to: (i) the lower availability of catalyst acid sites for oligomerization and side reactions; and, (ii) the diffusion limitations due to the presence of coke in the porous structure of the catalyst. Thus, the yields of higher molecular weight products (quantified as C_{5-7} and C_{5+} in Fig. 3d and e and 4d, e) decrease with time on stream, while the yields of the intermediate olefins, butenes (Fig. 3b and 4b) and propylene (Fig. 3a and 4a) increase. The growing trend in the yield of these olefins with time on stream indicates that catalyst deactivation affects in a major extent their oligomerization to higher olefins than their formation, by ethylene dimerization in the case of butenes and by β-scission of higher olefins in case of propylene (Fernandes et al., 2020, 2021). For the highest dilution (ethylene partial pressure in the feed of 0.33 bar), the constant yield of these olefins with time on stream can be attributed to a balance between the effect of deactivation on the reactions for their formation and conversion. The attenuation of the rate of hydrogen transfer reactions with catalyst deactivation is evidenced by the decrease of butane yield with time on stream (Fig. 3c and 4c), which is considered an index of the extent of these reactions, catalyzed by the acid sites of the HZSM-5 zeolite (Zhang et al., 2020).

Comparing the results with the two diluents in Figs. 3 and 4, the difference in the evolution of C_{5+} hydrocarbon yield with time on stream is striking. The lower initial yield and the less pronounced decrease of this yield with time on stream when syngas is used for dilution (Fig. 4e) in comparison to N_2 (Fig. 3e), is attributable to the greater attenuation of the extent of the reactions for aromatic formation by the presence of H_2, due to the shift of the dehydrocyclization reactions of olefins (Andrei et al., 2020). This result ratifies the role attributed to aromatics as coke precursors, which are responsible for catalyst deactivation (Mlinar et al.,
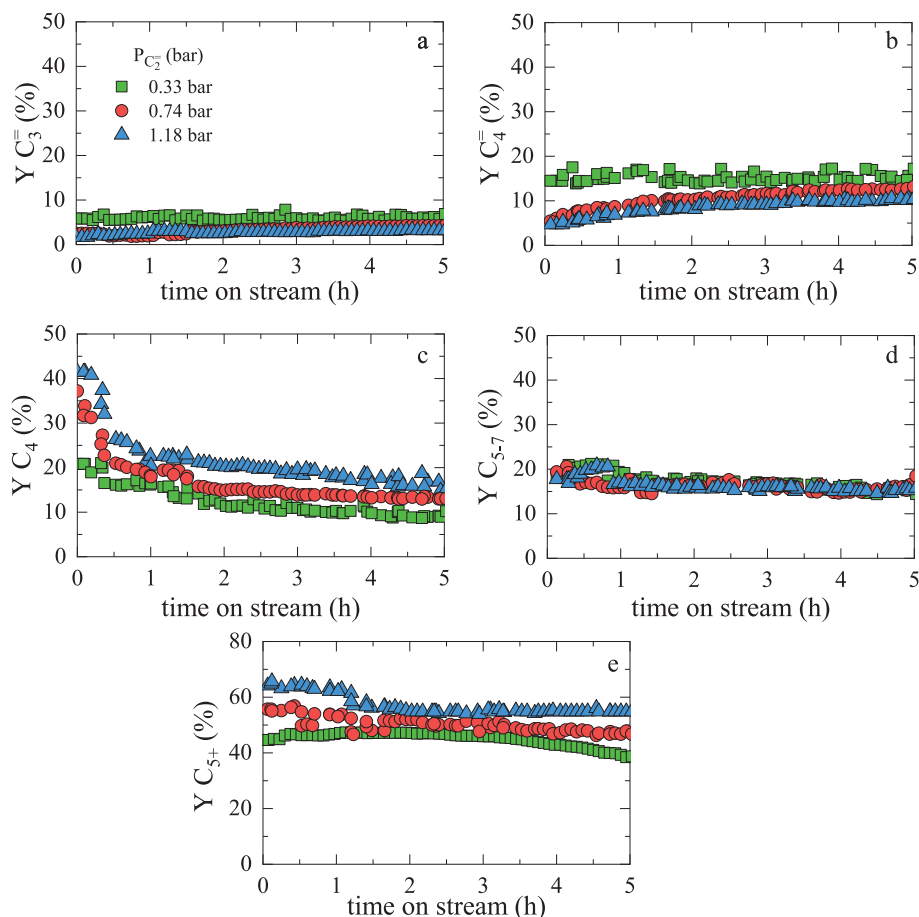
Fig. 3. Effect of ethylene partial pressure in the feed, using N_2 as diluent, on the evolution with time on stream of the main product yields: a) $C_3^=$, b) $C_4^=$, c) C_4, d) C_{5-7}, and e) C_{5+}. Reaction conditions: 325 °C; 1.5 bar; space time, 10.6 $g_{catalyst}$ h mol_C^{-1} (1 g of catalyst).

2012). Furthermore, the role of H_2 in attenuating the reaction extent of coke evolution towards condensed structures on acid catalysts is well established in some reactions where olefins participate as reactants or intermediates (Arora et al., 2018; Zhao et al., 2019).

3.3. Pseudo-state steady of the catalyst

For process scale-up, the results of product distribution in the catalyst pseudo-steady state (time on stream above of 3–4 h) are particularly interesting. These results are shown in Fig. 5, for the runs with N_2 (Fig. 5a) and syngas (Fig. 5b) as diluents. The higher conversion of ethylene in the pseudo-steady state with syngas as diluent is a consequence of the aforementioned (Section 3.2) lower deactivation with respect to the results with N_2 (Fig. 2), with a lower coke content in the catalyst when the equilibrium of its deposition is reached (as shown in Section 3.4). In addition, the presence of H_2 also justifies the lower yield of C_{5+} hydrocarbons, as the reactions for aromatic formation, which take place by olefin dehydrocyclization, are hindered (Andrei et al., 2020).

Figs. 6 and 7, corresponding to the runs with N_2 and syngas as diluents, respectively, show the selectivity of hydrocarbons (paraffins, olefins and aromatics) according to their carbon number, in the pseudo-steady state of the catalyst. The difference in the results with the two diluents is noteworthy. Thus, when N_2 is used (Fig. 6), as ethylene partial pressure increases and due to the greater extent of the reaction, the formation of hydrocarbons of higher molecular weight is favored, with a notable presence of C_{8+} hydrocarbons at a partial pressure of 1.18 bar. The higher selectivity of paraffins and aromatics with increasing ethylene partial pressure is also a consequence of the higher

extent of hydrogen transfer reactions. However, with syngas as diluent (Fig. 7) the effect of ethylene partial pressure is smaller. The suppression of the formation of C_{8+} hydrocarbons is to be highlighted, which can be explained by the attenuation of the extent of olefin dehydrocyclization, responsible for the formation of aromatics (Andrei et al., 2020; Fernandes et al., 2021). Considering the role attributed by Shi and Bhan (2022, 2023) to H_2 in the dual cycle mechanism of the conversion of methanol to olefins, the lower yield of aromatics and the higher yield of propylene and butenes with syngas dilution may be related to the participation of H_2 limiting the evolution of the aromatic cycle and favoring the formation of propylene and butenes from the olefin cycle. These authors also established that CO dilution only had an impact on the mechanism (for boosting the propagation of the aromatic cycle) at high pressure, which is also in agreement with the aforementioned results, that can be explained by the role of H_2.

3.4. Coke deposition

In Fig. 8 (N_2 dilution) and in Fig. 9 (syngas dilution), the N_2-TPS (graphs a) and TPO (graphs b) profiles for the corresponding used catalysts are shown. The contents of soft coke and hard coke indicated in these figures have been calculated from the area defined by the N_2-TPS and TPO profiles, respectively. The analysis conditions have been described in Section 2.3, and each profile corresponds to a type of coke (soft coke in N_2-TPS profile and hard coke in TPO profile). The existence of these two types of coke on the HZSM-5 zeolite catalysts in the oligomerization of ethylene is well established in the literature (Corma et al., 2013; Fernandes et al., 2020; Monama et al., 2020), where the rapid initial deactivation of the catalyst (observed in Fig. 2) is attributed
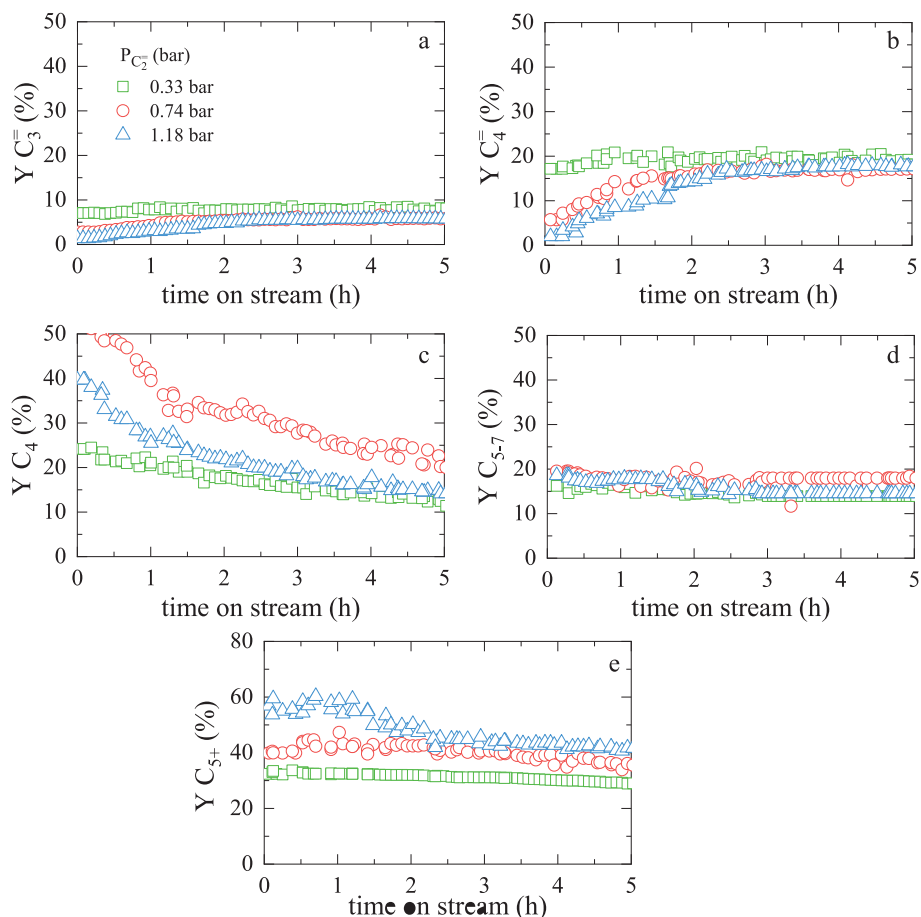
Fig. 4. Effect of ethylene partial pressure, using syngas as diluent, on the evolution with time on stream of the main product yields: a) $C_3^=$, b) $C_4^=$, c) C_4, d) C_{5-7}, and e) C_{5+}. Reaction conditions: 325 °C; 1.5 bar; space time, 10.6 $g_{catalyst}$ h mol_C^{-1} (1 g of catalyst).
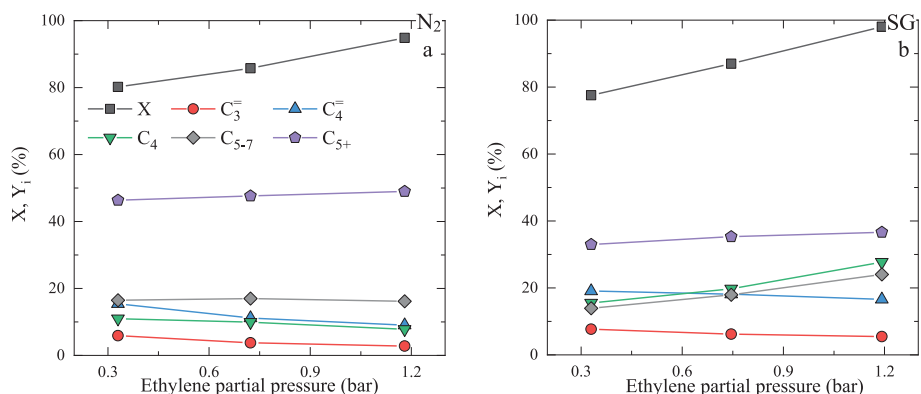

Fig. 5. Effect of ethylene partial pressure in the feed on its conversion and yields of the main lumped products in the pseudo-steady state of the catalyst, using as diluents, a) N_2 and b) syngas (SG). Reaction conditions: 325 °C; 1.5 bar; space time, 10.6 $g_{catalyst}$ h mol_C^{-1} (1 g of catalyst); 3 h on stream.

to the physical phenomenon of retention of the oligomers (soft coke) which partially block the zeolite micropores. Bickel and Gounder (2022) analyzed the diffusion limitations of the oligomers retained in the micropores of HZSM-5 zeolite and their effect on product distribution in the oligomerization of propylene. As shown in Fig. 2, after the initial rapid deactivation, the catalyst reaches a pseudo-steady state, at which a slow deactivation is observed, attributable to the formation and evolution of hard coke, with a lower incidence on catalyst pore blockage than soft coke retention (Jan et al., 2018).

For both diluents the content of soft coke is limited (Fig. 8a and 9a). Presumably the compounds are retained in the matrix of the catalyst, whose mesoporous structure allows their circulation throughout the reaction. Thus, a high fraction of soft coke present during each run is removed with the N_2 sweeping performed *in situ* at the end of each run (30 min at 325 °C). It is observed that the soft coke content increases with increasing ethylene partial pressure and the highest soft coke content of 1.8 wt% is obtained at an ethylene partial pressure of 1.18 bar. This reduced presence of soft coke justifies the catalyst to reach a pseudo-steady state in Fig. 2, with a remarkable remnant activity due to the fact that the access of ethylene and intermediates to the zeolite crystals is only partially limited. This effect of the hierarchical porous structure of attenuating the deposition of soft coke and its condensation
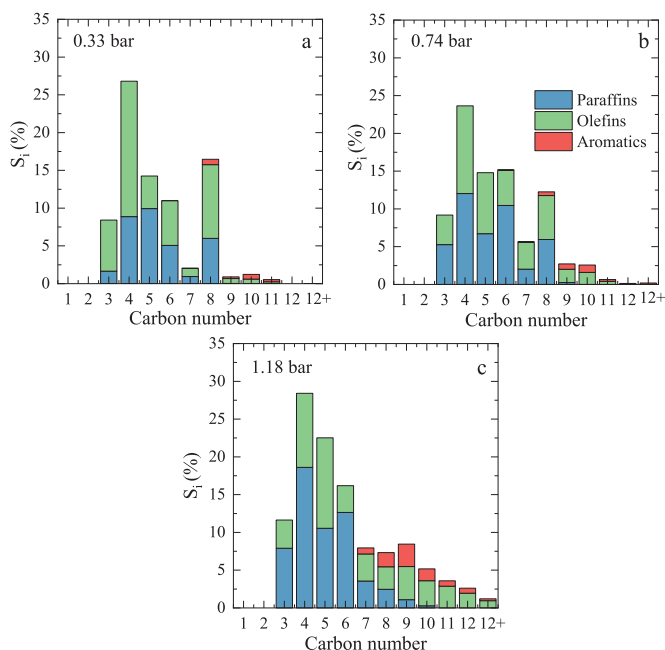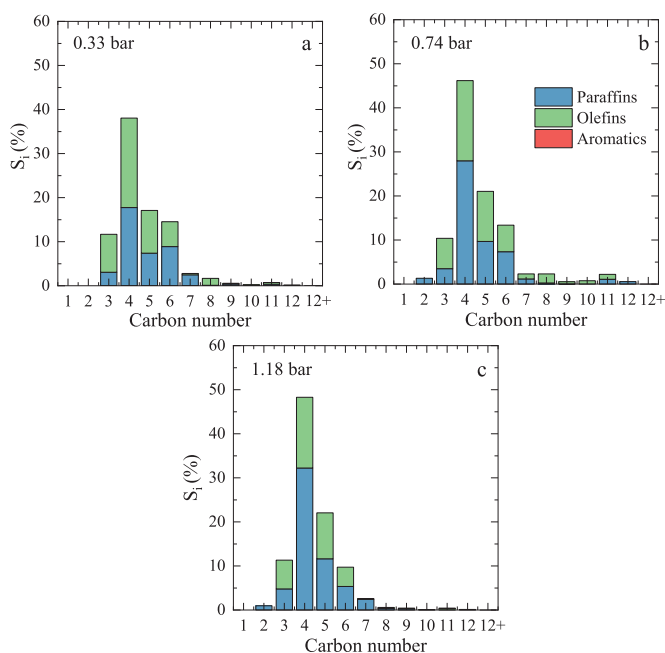
Fig. 6. Product distribution (selectivity) in the pseudo-steady state of the catalyst according to carbon number and hydrocarbon families (paraffins, olefins and aromatics) using N_2 as diluent at different ethylene partial pressure in the feed: a) 0.33 bar, b) 0.74 bar and c) 1.18 bar. Reaction conditions: 325 °C; 1.5 bar; space time, 10.6 $g_{catalyst}$ h mol_C^{-1} (1 g of catalyst); 3 h on stream.

Fig. 7. Product distribution (selectivity) in the pseudo-steady state of the catalyst according to carbon number and hydrocarbon families (paraffins, olefins and aromatics) using syngas as diluent at different ethylene partial pressure in the feed: a) 0.33 bar, b) 0.74 bar and c) 1.18 bar. Reaction conditions: 325 °C; 1.5 bar; space time, 10.6 $g_{catalyst}$ h mol_C^{-1} (1 g of catalyst); 3 h on stream.

reactions to hard coke has already been observed in the literature on catalysts prepared with a HZSM-5 with mesopores generated by desilication (Monama et al., 2020).

The mechanism of hard coke formation is slower than the fast retention of soft coke and takes place through reactions activated by the

acid sites of the catalyst (Halmenschlager et al., 2016; Zhang et al., 2020) where the dehydrocyclization of olefins and the hydrogen transfer reactions play a relevant role. The TPO profiles of the used catalysts (Fig. 8b and 9b) give evidence of the notable effect of increasing ethylene partial pressure, as hard coke content is boosted, whose maximum content is of 4.6 wt% for an ethylene partial pressure of 1.18 bar, with N_2 as diluent (Fig. 8b). For all the used catalysts, the TPO is deconvoluted into two characteristic peaks for the conversion of olefins over HZSM-5 zeolite catalysts, which are attributed to the combustion of two hard coke fractions (Ibáñez et al., 2017; Cordero-Lanzac et al., 2018; Díaz et al., 2021). The hard coke I, with the maximum combustion rate at ~460–480 °C, is likely deposited on the matrix and on the exterior of the crystals of the HZSM-5 zeolite, which facilitates its combustion. Hard coke II will be deposited inside the zeolite channels, by limiting air diffusion, which justifies the need for a higher combustion temperature, with a maximum rate at ~540–560 °C. The higher total hard coke content in the catalyst with increasing ethylene partial pressure is explained by the fact that the extent of the reactions for its formation are favored, in parallel to the higher extent of the reactions for the formation of higher hydrocarbons. The similar result obtained for the different diluents, with a maximum coke content of 5.3 wt% for a partial pressure of ethylene of 1.18 bar, suggests that coke formation does not occur directly from aromatics (absent in the reaction with syngas as diluent), but that its formation will take place by dehydrocyclization to polycondensed structures of the olefinic oligomers retained in the zeolite channels. This notable extent of olefin dehydrocyclization above 300 °C is well established (Bonnin et al., 2021). It is also noteworthy that the nature of the gaseous diluent shows a scarce incidence on coke evolution, because the coke II/coke I ratio (lower than 1 in all cases, in the 0.3–0.9 range) and the temperature of maximum combustion rate of these cokes (457–503 °C for coke I and 543–561 °C for coke II) show slight differences for these two diluents.

It should be highlighted that the coke features are suitable to facilitate catalyst regenerability (key condition for process scale up). Thus, the aforementioned results, with a high content of soft coke and a low condensed hard coke (regarding the temperature needed for its combustion) ease its removal. The procedure for catalyst regeneration has been established in a prior work (Díaz et al., 2021) for the same catalyst used in the oligomerization of 1-butene, which consists of two successive treatments, after which the full recovery of activity is obtained: i) sweeping with N_2 (1 h at 400 °C), for the removal of soft coke (trapped oligomers in the matrix), and; ii) subsequent combustion with air of the hard coke (mainly deposited on the zeolite micropores) (ramp of 10 °C min^{-1} between 400 and 500 °C and 0.5 h at 500 °C). Regarding that the coke deposited on this work in the oligomerization of diluted ethylene is less condensed, its removal with this treatment is also complete. Hence, the catalyst can be used in successive reaction-regeneration cycles.

4. Conclusions

The low-pressure oligomerization of ethylene diluted with N_2 or syngas enables to obtain a remarkable yield of higher hydrocarbons, which justifies the interest of developing a process for the valorization with low cost of secondary streams containing diluted ethylene. Thus, for an ethylene partial pressure of 0.33 bar the conversion of ethylene is greater than 80 % at 325 °C with either N_2 or syngas as diluents, for a moderate space time of 10.6 $g_{catalyst}$ h mol_C^{-1}, with a C_{5+} hydrocarbon yield higher than 40 % with N_2 and over 30 % with syngas. The reduced presence of aromatics with N_2 dilution, which is negligible with syngas, is also attractive for the obtained gasoline.

The presence of a mesoporous matrix in the HZSM-5 catalyst facilitates the diffusion of coke precursors, minimizing the problems of zeolite coke deactivation as the retention of the oligomers is limited, which facilitates the diffusion of soft coke (deposited in the matrix) and attenuates the hard coke formation reactions (mostly in the micropores of the HZSM-5 zeolite). This attenuation of coke deactivation is favored by
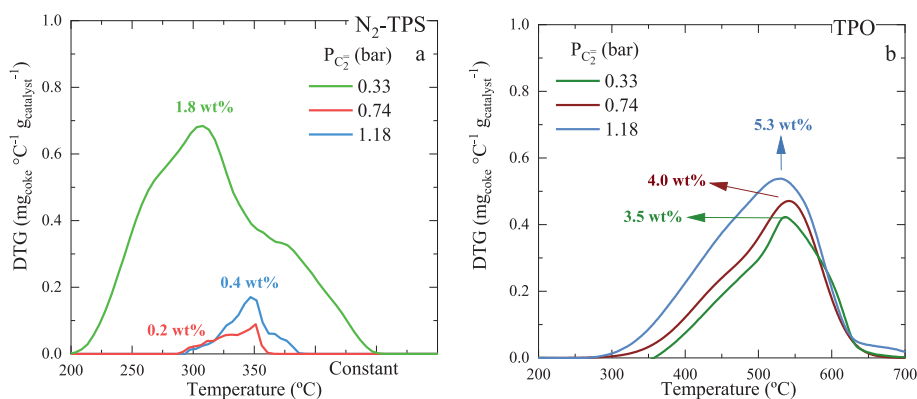
Fig. 8. Effect of ethylene partial pressure in the feed, using N_2 as diluent, on (a) N_2-TPS and (b) TPO profiles of the used catalysts. Reaction conditions: 325 °C; 1.5 bar; space time, 10.6 $g_{catalyst}$ h mol_C^{-1} (1 g of catalyst); 5 h on stream.
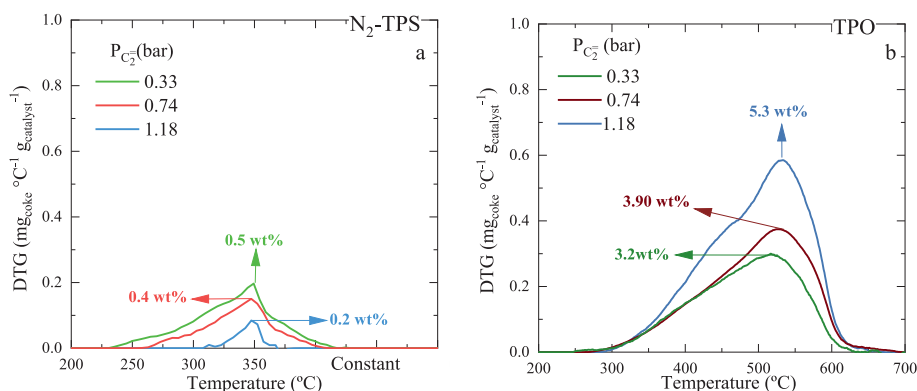

Fig. 9. Effect of ethylene partial pressure in the feed, using syngas as diluent, on (a) N_2-TPS and (b) TPO profiles of the used catalyst. Reaction conditions: 325 °C; 1.5 bar; space time, 10.6 $g_{catalyst}$ h mol_C^{-1} (1 g of catalyst); 5 h on stream.

the dilution of ethylene as the extent of coke formation is limited and the diffusion of the precursors (soft coke) from the retained coke is favored, which evolves in the crystalline channels of the zeolite (hard coke). Thus, the dilution of ethylene and the presence of the matrix in the catalyst contribute to maintaining a notable remnant activity after the initial stage of oligomer occlusion.

The results highlight the interest of low-pressure oligomerization of diluted ethylene to intensify the valorization of secondary streams from sustainable production processes of olefins and other hydrocarbons, yielding gasoline free of heteroatoms, and with a suitable composition to be added into the refinery gasoline pool.

Source of support

CRediT authorship contribution statement

Zuria Tabernilla: Data curation, Investigation, Methodology, Writing – original draft, Conceptualization, Writing – review & editing. **Ainara Ateka:** Validation, Visualization, Writing – original draft, Writing – review & editing, Conceptualization, Funding acquisition, Project administration. **Andrés T. Aguayo:** Methodology, Resources, Supervision, Data curation, Investigation, Validation. **Javier Bilbao:** Conceptualization, Data curation, Writing – original draft, Writing – review & editing, Supervision, Validation. **Eva Epelde:** Conceptualization, Data curation, Supervision, Writing – original draft, Writing – review & editing.

Declaration of competing interest

The authors declare that they have no known competing financial interests or personal relationships that could have appeared to influence the work reported in this paper.

Data availability

The authors are unable or have chosen not to specify which data has been used.

Acknowledgments

Appendix A. Supplementary data

Supplementary data to this article can be found online at https://doi.org/10.1016/j.jclepro.2024.141072.

References

Aguayo, A.T., Gayubo, A.G., Tarrío, A.M., Atutxa, A., Bilbao, J., 2002. Study of operating variables in the transformation of aqueous ethanol into hydrocarbons on an HZSM-5 zeolite. J. Chem. Technol. Biotechnol. 77, 211–216. https://doi.org/10.1002/jctb.540.

Andrei, R.D., Borodina, E., Minoux, D., Nesterenko, N., Dath, J.-P., Cammarano, C., Hulea, V., 2020. Ethylene oligomerization from diluted stream over Ni-containing heterogeneous catalysts. Ind. Eng. Chem. Res. 59, 1746–1752. https://doi.org/10.1021/acs.iecr.9b05576.

Arora, S.S., Nieskens, D.L.S., Malek, A., Bhan, A., 2018. Lifetime improvement in methanol-to-olefins catalysis over chabazite materials by high-pressure H_2 co-feeds. Nat. Catal. 1, 666–672. https://doi.org/10.1038/s41929-018-0125-2.

Artetxe, M., Lopez, G., Elordi, G., Amutio, M., Bilbao, J., Olazar, M., 2012. Production of light olefins from polyethylene in a two-step process: pyrolysis in a conical spouted bed and downstream high-temperature thermal cracking. Ind. Eng. Chem. Res. 51, 13915–13923. https://doi.org/10.1021/ie300178e.

Batchu, R., Galvita, V.V., Alexopoulos, K., Van der Borght, K., Poelman, H., Reyniers, M. F., Marin, G.B., 2017. Role of intermediates in reaction pathways from ethene to hydrocarbons over H-ZSM-5. Appl. Catal. Gen. 538, 207–220. https://doi.org/10.1016/j.apcata.2017.03.013.

Bickel, E.E., Gounder, R., 2022. Hydrocarbon products occluded within zeolite micropores impose transport barriers that regulate brønsted acid-catalyzed propene oligomerization. JACS Au 2, 2585–2595. https://doi.org/10.1021/jacsau.2c00462.

Bonnin, A., Pouilloux, Y., Coupard, V., Uzio, D., Pinard, L., 2021. Deactivation mechanism and regeneration study of Zn/HZSM-5 catalyst in ethylene transformation. Appl. Catal. Gen. 611, 117976 https://doi.org/10.1016/j.apcata.2020.117976.

Chen, G., Liu, H., Fadaeerayeni, S., Shan, J., Xing, A., Cheng, J., Wang, H., Xiang, Y., 2020. Tuning the reactivity of ethylene oligomerization by HZSM-5 framework Al proximity. Catal. Sci. Technol. 10, 4019–4029. https://doi.org/10.1039/d0cy00632g.

Chung, Y., Mores, D., Weckhuysen, B.M., 2011. Spatial and temporal mapping of coke formation during paraffin and olefin aromatization in individual H-ZSM-5 crystals. Appl. Catal. A Gen. 404, 12–20. https://doi.org/10.1016/j.apcata.2011.06.030.

Cordero-Lanzac, T., Ateka, A., Pérez-Uriarte, P., Castaño, P., Aguayo, A.T., Bilbao, J., 2018. Insight into the deactivation and regeneration of HZSM-5 zeolite catalysts in the conversion of dimethyl ether to olefins. Ind. Eng. Chem. Res. 57, 13689–13702. https://doi.org/10.1021/acs.iecr.8b03308.

Corma, A., Martínez, C., Doskocil, E., 2013. Designing MFI-based catalysts with improved catalyst life for $C_3^=$ and $C_5^=$ oligomerization to high-quality liquid fuels. J. Catal. 300, 183–196. https://doi.org/10.1016/j.jcat.2012.12.029.

Díaz, M., Epelde, E., Aguayo, A.T., Bilbao, J., 2020a. Low-pressure oligomerization of 1-butene to liquid fuels on HZSM-5 zeolite catalysts: effect of operating conditions. J. Ind. Eng. Chem. 87, 234–241. https://doi.org/10.1016/j.jiec.2020.04.006.

Díaz, M., Epelde, E., Tabernilla, Z., Ateka, A., Aguayo, A.T., Bilbao, J., 2020b. Operating conditions to maximize clean liquid fuels yield by oligomerization of 1-butene on HZSM-5 zeolite catalysts. Energy 207, 118317. https://doi.org/10.1016/j.energy.2020.118317.

Díaz, M., Epelde, E., Valecillos, J., Izaddoust, S., Aguayo, A.T., Bilbao, J., 2021. Coke deactivation and regeneration of HZSM-5 zeolite catalysts in the oligomerization of 1-butene. Appl. Catal., B 291, 120076. https://doi.org/10.1016/j.apcatb.2021.120076.

Ding, X., Geng, S., Liu, F, Y, Li, C.-Y., Yang, C.-H., 2009. Oligomerization of ethene on ZSM-5 catalyst. J. Fuel Chem. Technol. 37, 560–566.

Fernandes, D.S., Veloso, C.O., Henriques, C.A., 2020. Ethylene conversion into propylene and aromatics on HZSM-5: insights on reaction routes and water influence. Catal. Lett. 150, 738–752. https://doi.org/10.1007/s10562-019-02954-w.

Fernandes, D. da S., Oliveira Veloso, C. de, Henriques, C.A., 2021. Propylene and aromatics from ethylene conversion over ZSM-5: effect of zeolite composition. Catal. Today 381, 108–117. https://doi.org/10.1016/j.cattod.2020.08.014.

Garwood, W.E., 1983. Conversion of C_2-C_{10} to higher olefins over synthetic zeolite ZSM-5. ACS Symp. Ser. 218, 383–396. https://doi.org/10.1021/bk-1983-0218.ch023.

Gayubo, A.G., Tarrío, A.M., Aguayo, A.T., Olazar, M., Bilbao, J., 2001. Kinetic modelling of the transformation of aqueous ethanol into hydrocarbons on a HZSM-5 zeolite. Ind. Eng. Chem. Res. 40, 3467–3474. https://doi.org/10.1021/ie001115e.

Ghashghaee, M., 2018. Heterogeneous catalysts for gas-phase conversion of ethylene to higher olefins. Rev. Chem. Eng. 34, 595–655. https://doi.org/10.1515/revce-2017-0003.

Guisnet, M., Magnoux, P., 2001. Organic chemistry of coke formation. Appl. Catal. Gen. 212, 83–96. https://doi.org/10.1016/S0926-860X(00)00845-0.

Halmenschlager, C.M., Brar, M., Apan, I.T., de Klerk, A., 2016. Oligomerization of fischer–tropsch tail gas over H-ZSM-5. Ind. Eng. Chem. Res. 55, 13020–13031. https://doi.org/10.1021/acs.iecr.6b03861.

Ibáñez, M., Pérez-Uriarte, P., Sánchez-Contador, M., Cordero-Lanzac, T., Aguayo, A.T., Bilbao, J., Castaño, P., 2017. Nature and location of carbonaceous species in a composite HZSM-5 zeolite catalyst during the conversion of dimethyl ether into light olefins. Catalysts 7, 254. https://doi.org/10.3390/catal7090254.

Jan, O., Song, K., Dichiara, A., Resende, F.L.P., 2018. Ethylene oligomerization over Ni–Hβ heterogeneous catalysts. Ind. Eng. Chem. Res. 57, 10241–10250. https://doi.org/10.1021/acs.iecr.8b01902.

Jin, F., Zhang, P., Wu, G., 2021. Fundamental kinetics model of acidity-activity relation for ethylene oligomerization and aromatization over ZSM-5 zeolites. Chem. Eng. Sci. 229, 116144 https://doi.org/10.1016/j.ces.2020.116144.

Johansson, R., Hruby, S.L., Rass-Hansen, J., Christensen, C.H., 2009. The hydrocarbon pool in ethanol-to-gasoline over HZSM-5 catalysts. Catal. Lett. 127, 1–6. https://doi.org/10.1007/s10562-008-9711-2.

Kriván, E., Tomasek, S., Hancsók, J., 2016. The oligomerization of high olefin containing hydrocarbon by-products to clean engine fuels. J. Clean. Prod. 136, 81–88. https://doi.org/10.1016/j.jclepro.2016.06.020.

Li, C., Wang, H., Zhu, S.S., Liu, G.B., Wu, J.H., 2017. Research on butene oligomerization reaction over the hemicellulose modified HZSM-5. J. Fuel Chem. Technol. 45, 1088–1094. https://doi.org/10.1016/S1872-5813(17)30051-8.

Lin, B., Zhang, Q., Wang, Y., 2009. Catalytic conversion of ethylene to propylene and butenes over H-ZSM-5. Ind. Eng. Chem. Res. 48, 10788–10795. https://doi.org/10.1021/ie901227p.

Liu, J., Yue, J., Lv, M., Wang, F., Cui, Y., Zhang, Z., Xu, G., 2022. From fundamentals to chemical engineering on oxidative coupling of methane for ethylene production: a review. Carbon Resources Conver 5, 1–14. https://doi.org/10.1016/j.crcon.2021.11.001.

Mlinar, A.N., Zimmerman, P.M., Celik, F.E., Head-Gordon, M., Bell, A.T., 2012. Effects of Brønsted-acid site proximity on the oligomerization of propene in H-MFI. J. Catal. 288, 65–73. https://doi.org/10.1016/j.jcat.2012.01.002.

Moioli, E., 2022. Process intensification and energy transition: a necessary coupling? Chem Eng Process Process Intensif 179, 109097. https://doi.org/10.1016/j.cep.2022.109097.

Monama, W., Mohiuddin, E., Thangaraj, B., Mdleleni, M.M., Key, D., 2020. Oligomerization of lower olefins to fuel range hydrocarbons over texturally enhanced ZSM-5 catalyst. Catal. Today 342, 167–177. https://doi.org/10.1016/j.cattod.2019.02.061.

Palos, R., Gutiérrez, A., Fernández, M.L., Azkoiti, M.J., Bilbao, J., Arandes, J.M., 2020. Converting the surplus of low-quality naphtha into more valuable products by feeding it to a fluid catalytic cracking unit. Ind. Eng. Chem. Res. 59, 16868–16875. https://doi.org/10.1021/acs.iecr.0c03257.

Pérez Uriarte, P., Gamero, M., Ateka, A., Díaz, M., Aguayo, A.T., Bilbao, J., 2016. Effect of the acidity of HZSM-5 zeolite and the binder in the DME transformation to olefins. Ind. Eng. Chem. Res. 55, 1513–1521. https://doi.org/10.1021/acs.iecr.5b04477.

Portillo, A., Ateka, A., Ereña, J., Aguayo, A.T., Bilbao, J., 2022. Conditions for the joint conversion of CO_2 and syngas in the direct synthesis of light olefins Using In_2O_3-ZrO_2/SAPO-34 Catalyst. Ind. Eng. Chem. Res. 61, 10365–10376. https://doi.org/10.1021/acs.iecr.1c03556.

Quann, R.J., Green, L.A., Tabak, S.A., Krambeck, F.J., 1988. Chemistry of olefin oligomerization over zsm-5 catalyst. Ind. Eng. Chem. Res. 27, 565–570. https://doi.org/10.1021/ie00076a006.

Rissman, J., Bataille, C., Masanet, E., Aden, N., Morrow, W.R., Zhou, N., Elliott, N., Dell, R., Heeren, N., Huckestein, B., Cresko, J., Miller, S.A., Roy, J., Fennell, P., Cremmins, B., Koch Blank, T., Hone, D., Williams, E.D., de la Rue du Can, S., Sisson, B., Williams, M., Katzenberger, J., Burtraw, D., Sethi, G., Ping, H., Danielson, D., Lu, H., Lorber, T., Dinkel, J., Helseth, J., 2020. Technologies and policies to decarbonize global industry: review and assessment of mitigation drivers through 2070. Appl. Energy 266, 114848. https://doi.org/10.1016/j.apenergy.2020.114848.

Shi, Z., Bhan, A., 2022. Methanol-to-olefins catalysis on window-cage type zeolites/zeotypes with syngas co-feeds: understanding syngas-to-olefins chemistry. J. Catal. 413, 913–922. https://doi.org/10.1016/j.jcat.2022.07.035.

Shi, Z., Bhan, A., 2023. The effects of CO co-feed on the catalytic performance of Methanol-to-Hydrocarbons conversion on HZSM-5. Chem. Eng. J. 456, 140867 https://doi.org/10.1016/j.cej.2022.140867.

Tabak, S.A., Krambeck, F.J., Garwood, W.E., 1986. Conversion of propylene and butylene over ZSM-5 catalyst. AIChE J. 32, 1526–1531. https://doi.org/10.1002/aic.690320913.

Tabernilla, Z., Ateka, A., Bilbao, J., Aguayo, A., Epelde, E., 2023. Performance of HZSM-5 agglomerated in a mesoporous matrix in the fuel production from ethylene at atmospheric pressure. Energy 284, 128703. https://doi.org/10.1016/j.energy.2023.128703.

Van der Borght, K., Batchu, R., Galvita, V.V., Alexopoulos, K., Reyniers, M.F., Thybaut, J. W., Marin, G.B., 2016. Insights into the reaction mechanism of ethanol conversion into hydrocarbons on H-ZSM-5. Angew. Chem. Int. Ed. 55, 12817–12821. https://doi.org/10.1002/anie.201607230.

Zeng, S., Zhang, W., Li, J., Lin, S., Xu, S., Wei, Y., Liu, Z., 2022. Revealing the roles of hydrocarbon pool mechanism in ethanol-to-hydrocarbons reaction. J. Catal. 413, 517–526. https://doi.org/10.1016/j.jcat.2022.07.002.

Zhang, J., Tang, R., Shen, Z., Liang, S., Zhong, H., 2020. Catalytic oligomerization of ethylene over nano-sized HZSM-5. J. Energy Inst. 93, 2550–2557. https://doi.org/10.1016/j.joei.2020.09.002.

Zhang, Z., Hu, G., Mu, X., Kong, L., 2022. From low carbon to carbon neutrality: a bibliometric analysis of the status, evolution and development trend. J. Environ. Manag. 322, 116087 https://doi.org/10.1016/j.jenvman.2022.116087.

Zhao, X., Li, J., Tian, P., Wang, L., Li, X., Lin, S., Guo, X., Liu, Z., 2019. Achieving a superlong lifetime in the zeolite-catalyzed MTO reaction under high pressure: synergistic effect of hydrogen and water. ACS Catal. 9, 3017–3025. https://doi.org/10.1021/acscatal.8b04402.